

Chapter 10

Flow Simulation of a New Horizontal Axis Wind Turbine with Multiple Blades for Low Wind Speed



Essam Abo-Serie and Elif Oran

Abstract In this paper, a new design of a small horizontal-axis wind turbine is introduced. The design is based on the authors' patent, which uses permanent magnets impeded into a shroud that holds the rotor blades. The generator coils are installed on a fixed diffuser that houses the rotor and acts as a wind concentrator. Therefore, the new design has no hub and is based on direct coupling for electricity generation. The main features of the design have been explored to highlight the advantages with a focus on how the new design can be integrated with the recent development of green buildings. The effect of increasing the number of blades and blade chord distribution on turbine performance has been investigated for the new turbine. Initial design and analysis were carried out using the Blade Element Momentum method and CFD simulations to identify the turbine performance and examine the flow characteristics. The results showed that further energy can be extracted from the turbine if the blade chord size increases at the shroud location and reduces at the turbine hub for a low Tip Speed Ratio TSR within the range of 1.5–3. Furthermore, having more blades can significantly increase the power coefficient and extend the range of operation with a high power coefficient. The number of blades, however, has to be optimised to achieve maximum power relative to the cost. Adding a diffuser and flanges surrounding the turbine can further increase the energy extracted from the wind at low speed.

Keywords Wind energy · Wind power · Small wind turbines · Shrouded wind turbine · Magnetic levitated wind turbine blades

E. Abo-Serie (✉)
School of Engineering, University of Leicester, Leicester, UK
e-mail: e.aboserie@leicester.ac.uk

E. Oran
School of Mechanical Automotive and Aerospace Engineering, Coventry University, Coventry, UK

10.1 Introduction

There is a growing interest in using clean renewable energy resources due to recent energy demand and increasing energy prices. Moreover, a tendency toward clean renewable energy resources like wind, solar, and hydro has increased because of environmental pollution. Investment, thus, has considerably increased in wind energy over the last decade. In addition, nowadays smart buildings that produce their own power have also become very popular. Integrating renewable sources of green energy with new buildings is among the priority areas in the United States and Europe under the “Green Building” concept. Many small wind turbines are now available in the market and used in residential, agricultural, small commercial farm applications, remote communication stations, and industrial applications, either grid-connected or off-grid, using batteries for energy storage. To spread the use of small wind turbines, their drawbacks have to be limited or eliminated, particularly their limited power generation at low wind speed. The aerodynamic and mechanical noises are also major concern for small turbines to be used in residential areas [1]. More challenging; is the ability to operate efficiently micro wind turbines in urban environments and buildings [2].

Small wind turbines that operate in low-wind environments are prone to suffer performance degradation as they often fail to accelerate to a steady, power-producing condition. Flow separation at the leading-edge occurs at low Reynolds number and high attack angle, leading to sudden stall and, consequently, power loss. Previous studies showed that the design of aerofoil is critical to achieving a better start with a recommendation to use mixed-aerofoils. The improved starting capability effectively reduces the time that the turbine takes to reach its power-extraction period and, hence, an increase in overall energy, which can be as much as 40% of the generated energy [3]. Moreover, small turbines have low start-up torque because of their short rotor diameter and blade length. The power coefficient for this type of wind turbine can be about 0.25, much lower than their large counterparts with a power coefficient of 0.45 [4]. In urban areas, wind turbines typically operate at Reynolds numbers lower than 5×10^5 due to their small rotor diameter, leading to reduced aerofoil's chord size [5]. The aerodynamics characteristic of the rotor aerofoil is a key factor that mostly affects the performance coefficient of turbines [6].

To overcome the drawback of small wind turbines, there has been continuing interest in concentrating wind flow into the turbine with the use of a smaller, lighter, and faster rotor to extract as much energy as that from a large rotor in open flow [7]. The typical way of concentrating the wind is by placing the rotor in a duct or diffuser, which allows extra mass to pass through the rotor compared to an open flow [8]. Concentrating the wind speed can reduce the ‘cut-in speed’, a wind speed below which the blades do not turn. According to Generalized Actuator Disc (GAD) method that considers a flow concentration device, the extracted energy from the wind can exceed the well-known Betz limit which is based on an open flow system. That increase is proportional to the flow augmentation achieved by the diffuser. With the GAD method, it is proved that the energy extracted by the rotor can reach as much

as 8/9 of the upstream wind energy [7, 9]. With some mathematical manipulation for the GAD method, and the Blade-Element Momentum method [10, 11], the blade twisting for the maximum lift-to-drag ratio can be identified. However, it is important to keep in mind that these methods are developed based on 2-D and inviscid flow and therefore, various correction factors have to be applied [12].

Further research work on using a shrouded turbine led to the use of a flange at the end of the diffuser [13–15]. The flange generates vortices downstream of the turbine blades causing a low-pressure zone that accelerates the flow through the turbine blades leading to a significant increase in the air mass flow rate. With the use of a large flange on a 500 W turbine, it was reported that the extracted power could be up to five times the power of an open wind turbine [16]. The use of a blade-shroud suppresses the vortices generated from the blade tips through the interference with the diffuser shroud boundary layer and therefore leads to a substantial reduction in the aerodynamic noise [17]. The shrouded structure is also providing safety toward possible damage to the blades upon hitting the tower [16]. In spite of the advantages the shrouded turbine can provide, there are challenges that need to be tackled for the shroud to be widely used and accepted. The main challenges are the extra cost and weight due to the material and manufacturing of the shroud surrounding the turbine blades. Moreover, the shrouded flanged turbine leads to higher blade speed which adds extra load on the wind turbine supporting the structure [18]. In order to limit the load and cost, the use of a short-flanged diffuser has been attempted by many researchers [19]. More recent research showed numerically that the use of a self-adaptive flange could reduce the wind load acting on the diffuser by 34.5% [20].

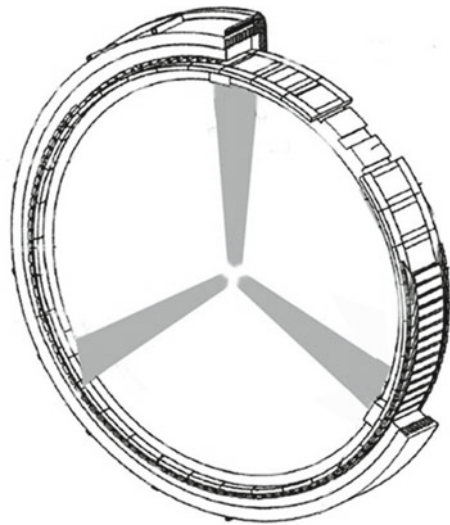
The effort to improve the performance of the wind turbine is not only limited to aerodynamics but also includes some changes in the architecture of the wind turbine system [21]. The wind generators are commonly coupled to a gearbox to transfer low-speed and high torque rotors to the generator. However, recent technology development removed the gearbox using a direct driver generator. The gearbox is not only costly but also needs regular maintenance and negatively affects the system efficiency. It is expected that further improvement will be carried out towards the direct coupling techniques with the further development in power electronics. In this work, a further improvement in the turbine design is proposed that can further increase the extracted power of the turbine, particularly for small size, and simplify the design with a more rigid structure. The proposed design uses a suspended shrouded rotor with permanent magnets impeded in the turbine shroud while the stator, which is part of the diffuser, carries the generator coils. The new design has a higher relative velocity between the rotor and stator and can have multiple coils; therefore, there is no need to have a gearbox. Moreover, the blades are no longer connected to a central hub but instead on the shroud of the rotor. The work shown here will provide a numerical analysis of how the new design can deliver more power than the conventional design.

10.2 New Design Approach

In the current design, the turbine blades are connected through a shroud; therefore, there is no need for a hub. Moreover, it can have more blades arranged in many different ways to achieve the best performance. Having more blades and no central hub can improve the efficiency of the turbine based on Betz's theory of wind machines [11]. The theory is based on assuming a turbine with an infinite number of rotor blades that do not result in any drag resistance to the wind flowing through them. The new turbine may have the rotor suspended by the magnetic field and therefore, there is no metal-to-metal contact or lubricant oil between the rotor and stator. This design, therefore, eliminates the mechanical noises. Furthermore, the blade can be made rigid enough without worrying about the turbine hub size. Moreover, it can easily be integrated into a diffuser to concentrate the wind that path through the blades. The turbine can be part of any building or civil construction work without a need for a special structure, as shown in Fig. 10.1. The blades are more secure as there is no way to have blades hitting the tower. The main advantages of the new design relative to the conventional turbine can be summarised as follow:

- Low wind noise as there is no clearance between the blade tip and diffuser.
- Mechanical noise due to friction is eliminated as the rotor is magnetically suspended.
- Lower stress is acting on the blade roots as the wind forces acting near the hub of the turbine are minimum.
- Rotor blades can be made more rigid and lighter.
- Rotor with multiple blades can be used.
- Efficiency is improved due to direct coupling and removal of the gearbox.

Fig. 10.1 Proposed wind turbine design



- High torque can be generated at low wind speed. The pressure difference between the two sides of the aerofoil near the tip will produce high force and torque due to its relatively larger area and longer radius.
- There is more flexibility in blade shape design.
- The drawback of small size turbines in terms of noise can be eliminated using a suspended rotor.

Although these mentioned advantages can logically be explained, work is currently carried out to evaluate and maximise the benefits. It is also equally important to evaluate the drawbacks of the new design, particularly in terms of power density and cost.

10.3 Operating Parameters and Methodology

This work pays attention to two major parameters that can improve the turbine aerodynamic performance. The first parameter is chord distribution along the blade length and the second parameter is the number of blades. A small turbine of a diameter 4.3 m using NREL S822 aerofoil is used in this investigation. Detail of the operating conditions and main geometry is shown in Table 10.1 and Fig. 10.2. For BEM method, six different designs have been investigated. The first one has a chord length that is linearly increased from a minimum value C_{\min} at the hub to a maximum C_{\max} at the tip and has three blades. The second turbine also has three blades, but the chord length is inversely laid down where the large chord length is located at the tip and the smallest at the hub. The other three designs are similar to the second design but have 5, 8, 12 and 18 blades. The solidity of 3, 5, 8, 12 and 18 blades is 0.08, 0.13, 0.21, 0.32 and 0.49 respectively. The wind speed is varied from 2 to 16 m/s and tip speed ratios from 0.5 to 4. The different cases that have been analysed are shown in Fig. 10.3. The turbine shroud and concentrator have only been used in the CFD simulation to examine the effect of increasing the wind speed on the extracted power.

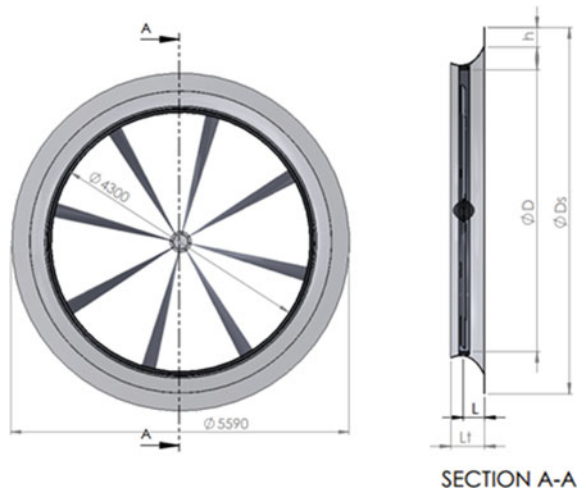
Blade Element Momentum Method

The design was carried out using BEM method which is the common method used in industry to provide the initial design of wind turbines. Although this method is developed for 2-D flow its results are reliable after the correction factors are applied [12]. Detail about the method and the derived equations can be found in many references [22]. The NREL S822 profile is used in Q-blade software [23] to carry out the BEM analysis. Based on the BEM method, the blade is divided radially into eight sections, and the values of axial induction factor (a) and tangential induction factor (a') are calculated using an iterative method from the drag and lift coefficients of the blade at each section. The pitch angle of the blade can then be calculated at each section along the blade for a specific tip speed ratio [22]. The velocity triangle at the tip of the blade is shown in Fig. 10.4; similar triangles can be drawn at each of the eight sections of the turbine blade which has a different value of blade speed.

Table 10.1 The main parameters used in the CFD simulation

Parameter	Unit	Symbol	
Wind velocity (V_o)	m/s	V	7
Rotational speed	Rpm	n	75
Diameter $D = 2R$	M	D	4.3
Tip blade speed	m/s	U	16.89
Tip speed ratio		TSR	2.41
Hub diameter	Cm	d	30
Min. chord length	Cm	C_{min}	5
Max. chord length	Cm	C_{max}	25
Blade number		Z	3,5,12,18
Blade length	M	L_b	2
Shroud diameter	M	D_s	1.3 D
The width of the brim	M	h	0.15 D
The diffuser length	M	L_t	1.47 D

Fig. 10.2 Main dimensions of the diffuser and shroud used in the study



Computational Fluid Dynamics

This work also examines the 3-D flow pattern and the energy transmitted to the wind turbine blades using the commercial package STARCCM + version 10.04. Only the 8-blade turbine is investigated using CFD, considering a surrounded short diffuser and flange. The aim is to evaluate the percentage increase of power from the wind concentrator. The flow was assumed to be steady and incompressible since Mach number is approximately 0.03 which is much below to affect the density value. Reynolds Averaged Navier Stokes, RANS equations are employed together with the SST k-ε turbulence model equations to identify the flow pattern within the flow

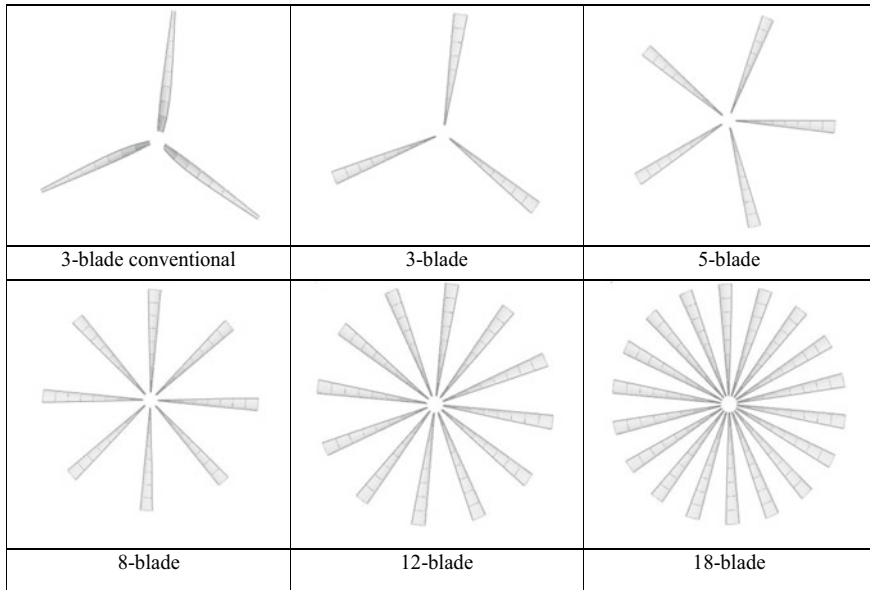


Fig. 10.3 Turbine baseline and the new turbine with different blades number

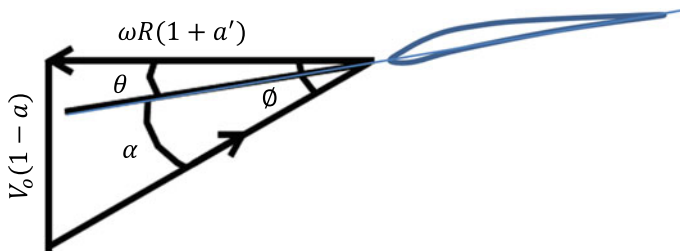


Fig. 10.4 Sketch showing the velocity triangle at the tip of the blade

domain. The SST $k-\epsilon$ model was selected based on previous studies, which showed the predicted results were close to the experimental data [24]. A rotating reference frame was employed to represent the rotation of the fluid region of the rotor.

The computation domain consists of a cylindrical segment that contains a single blade and part of the hub, shroud and the surrounded cylinder. The segment size for the 8-blade turbine has an angle of 45° . A periodic boundary condition is applied on the two sides of the segment. The domain is separated into two subdomains; the first is the rotating region which includes the rotating blades and a shroud, and the second subdomain contains the outer region, as shown in Fig. 10.5. The outer region has a length of five times the turbine radius downstream the turbine and a radius equal to 2.5 times the turbine radius. A uniform, steady velocity is assumed at the inlet of the computational domain with 5% turbulence intensity. The pressure outlet

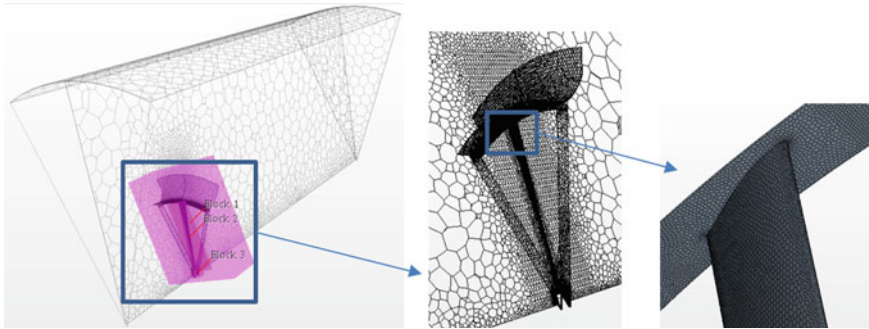


Fig. 10.5 The polyhedral mesh with refining zones and blade surface refined mesh

boundary condition is applied at the outlet. A symmetrical wall boundary condition is applied across the curved cylinder segment surface of the outer domain. For all turbine surfaces, a no-slip boundary condition is specified.

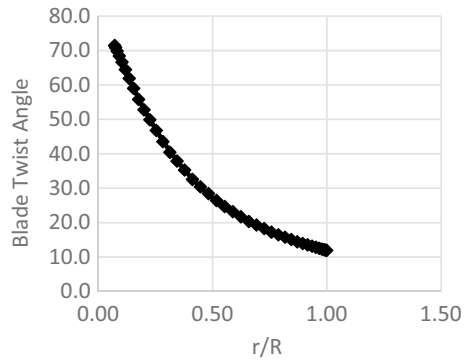
Figure 10.5 also shows the unstructured polyhedral mesh that is used in the computation domain with a refined mesh size in the rotating region and where a high-velocity gradient is expected. The effect of having different ways of refining the mesh can influence the simulation error [25]. In this study, different volumetric control zones have been selected and refined based on the expected velocity gradient while mesh size ratio expansion is set to slowly change the mesh size from the zone of large size mesh to the small size mesh. Special attention is paid to the mesh on the surface of the blades to keep the edges during the volume meshing. Prism layers are used around the surface of the turbine to accurately calculate the shear force and adjust y^+ value to be within the recommended values of 30–100 in order to have the first cell adjacent to the wall located within the logarithmic region of the boundary layer.

10.4 Results and Discussions

Blade Element Momentum Results

After the blade aerofoil is identified, the lift and drag coefficients have been estimated for various attack angles using XFOIL algorithm, which is implemented in QBlade software [26]. The evaluated drag and lift coefficients were found to be close to the values tabulated by NREL. The maximum lift-to-drag ratio was found to be at 6° . The optimum twist angle was calculated for each section for a tip speed ratio of 2.4. This value was chosen to allow the turbine to be used at low wind speed. The values of the twist angle along the blade radius are shown in Fig. 10.6. With the new blades, the twisting is not difficult since the high twist occurs near the hub, where the chord size is small.

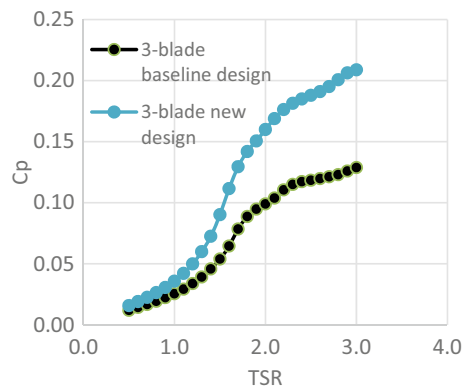
Fig. 10.6 Blade twist angle along the blade radius



A comparison between the new chord distribution blade and the conventional blades is shown in Fig. 10.7. The power coefficient C_p for the new blade design is significantly more than the conventional blade with almost 36% at TSR of 2.4 for the 3-blade turbine. This value increases to 61% at TSR of 3. This is not a surprise since the interaction property between the fluid and the blades is the pressure, and having a large area toward the tip will increase the force which is multiplied by a long radius to produce the torque. The linear increase of the blade chord size is not the optimum profile, but it is selected here to simplify the model and to prove the concept.

In order to examine how the number of blades or solidity affects the turbine performance, the power coefficient has been evaluated for different blade numbers and TSR, as shown in Fig. 10.8. The figure shows significantly improved C_p values as the blade number increases. It also shows that the range of operation at high C_p values increases with the number of blades. In other words, the wind turbine can work with a high power factor over a broader range of wind speeds if the turbine speed remains constant. The figure also indicates that the turbine with more blades can work more efficiently at low wind speeds. It is also noticeable that the maximum

Fig. 10.7 Blade power coefficient at different tip speed ratio for the new and conventional blades



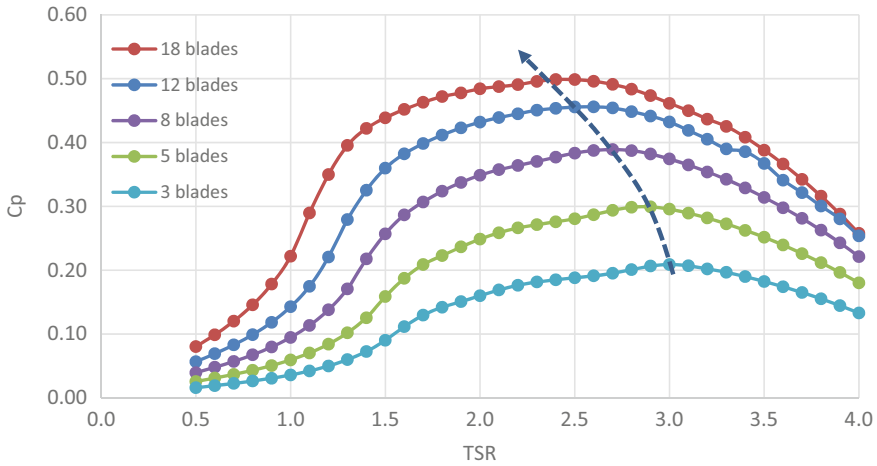


Fig. 10.8 Effect of blade number on power coefficient for the new blades

value of C_p is shifted towards lower TSR as the blade number increases. For $TSR = 1$, the value of C_p for the 18-blade turbine is almost five times that of the 3-blade turbine. Almost the same ratio can be found at $TSR = 1.5$.

Since the speed of the small turbine can be varied based on the wind speed, it is possible to keep the TSR at its optimum value. Figure 10.9 shows how the wind power does not change considerably with the TSR compared to the change if TSR is kept at its optimum value.

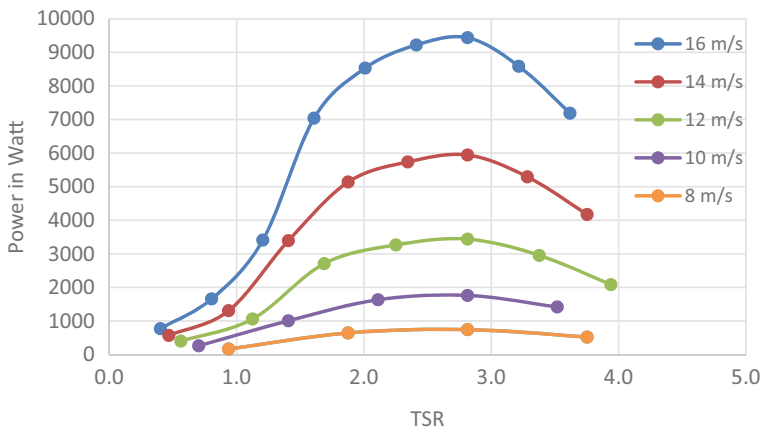


Fig. 10.9 Effect of wind speed on the generated power for the 8-blade turbine

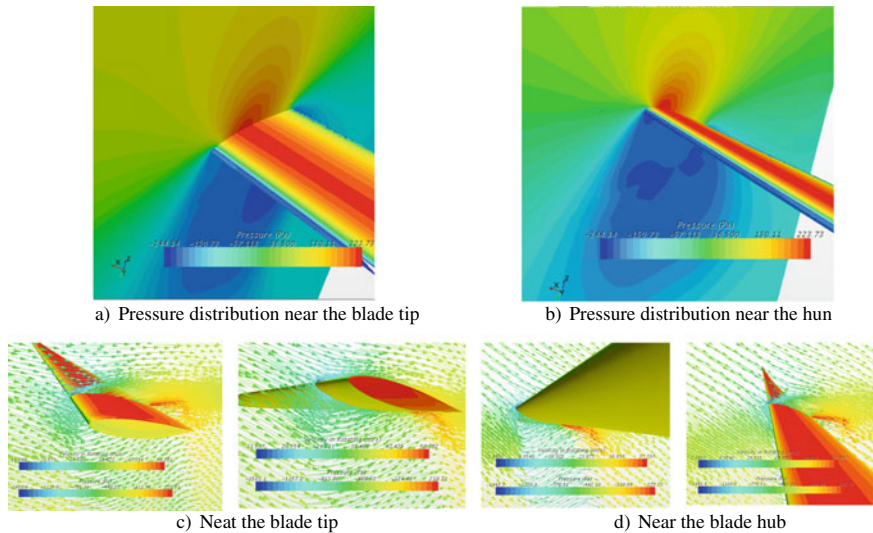


Fig. 10.10 Flow velocity and blade pressure distribution near and tip and hub of the blade

CFD Results

In order to demonstrate the effect of using a shroud and flange on the turbine to concentrate the wind and increase the spatial distribution of velocity and pressure were evaluated using the CFD simulation. The velocity vector around the blade was first investigated to examine the existence of flow separation around the blade. Figure 10.10 shows an attached flow near the tip of the blade and the pressure distribution at the back and front sides of the blades. From the figure, it can be seen that the values of the pressure near the hub and tip are almost the same. However, due to the larger surface area near the blade tip, a larger torque and consequently more power can be produced.

The effect of blade turbine shroud and flanges on flow pattern and pressure is shown in Fig. 10.11. A large vortex is formed behind the shroud flange generating a low-pressure region that extends downstream of the turbine by a distance almost equal to the blade radius. The location of the low-pressure region depends on the flange design. Nevertheless, the low-pressure region assists in driving more air to pass through the turbine blades and consequently increases the generated power. The turbine power is evaluated by integrating the torque over the turbine blade surface area, considering both the pressure and shear stress. The integrated torque was calculated for three wind speeds: 8, 12 and 16 m/s, while keeping the TSR at its optimum value of 2.41; therefore, the turbine rotational speed changes to 75, 130 and 172 rpm, respectively. The calculated torque is multiplied by the angular speed of the blades to evaluate the transmitted power. The power obtained using CFD for the flange and diffuser turbine is compared with the power calculated using the BEM method for the open turbine, as shown in Fig. 10.12. Adding the flange to the

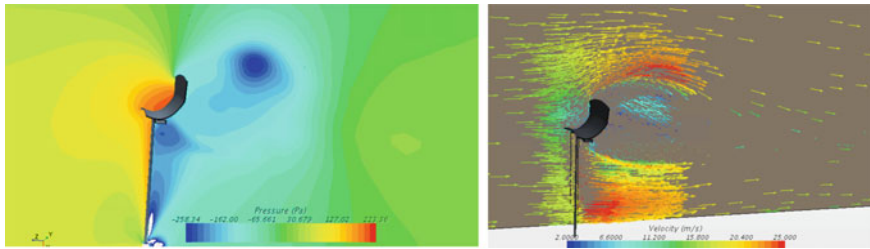


Fig. 10.11 Flow pressure and velocity vector distribution along a plan showing the effect of the shroud and flange on flow distribution

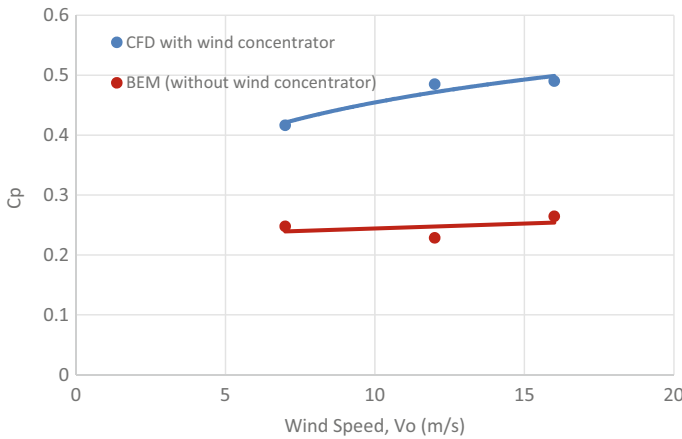


Fig. 10.12 The effect of the concentrator on the power coefficient relative to the value calculated using BEM method for a bare turbine at $TSR = 2.41$

shroud stator has a significant improvement in C_p value which may exceed the Bitz limit after optimising the flange geometry and the wind concentrator at low TSR. The increase of C_p value with wind speed may be attributed to the further drop in pressure in the wake region. Currently, experimental work is carried out to test a prototype.

10.5 Conclusions

A new innovative design for a small axial wind turbine that has a suspended rotor surrounded by a permanent magnet has been introduced. The performance has been explored considering inversely laid blades and having more blades. Using the BEM method and CFD simulation, it has conceptually proved that the newly designed turbine with a blade chord length increasing towards the tip can run at lower wind

speed and extract more power from the wind. Furthermore, increasing the number of blades can extend its range of operation to lower wind speeds and improve the power coefficient. Finally, the CFD results showed that adding a small size diffuser with a flange can concentrate the wind and therefore improve the aerodynamic performance of the wind turbine.

References

1. N. Prabakaran, K.J. Krishnan, S. Dhamodharan, Design and analysis of horizontal axis wind turbine blade. *Int. J. Inf. Technol. Comput. Sci. Perspect.* **2**(1), 435–444 (2013)
2. Encraft Organization, ‘Warwick Microwind Trial project’ final Report, at <http://www.warwickkwindtrials.org.uk/resources/Warwick+Wind+Trials+Final+Report+.pdf>. Accessed on 13 June 2022
3. S. Worasinchal, Small Wind Turbine Starting Behaviour, Durham theses, Durham University, 2012. Available at Durham E-Theses Online: <http://etheses.dur.ac.uk/4436/>
4. R.K. Singh, M. Rafiuddin Ahmed, M. Asid Zullah et al., Design of a low reynolds number airfoil for small horizontal axis wind turbines. Elsevier, *Renew. Energy* **42**, 66–76 (2012)
5. R.K. Singh, M. Rafiuddin Ahmed, Blade design and performance testing of a smallwind turbine rotor for low wind speed applications. Elsevier, *Renew. Energy* **50**, 812–819 (2013)
6. J. Yao, W. Yuan, Wang et al., Numerical simulation of aerodynamic performance for two dimensional wind turbine airfoils. Elsevier, *Energy Proc.* **31**, 88–86 (2012)
7. P. Jamieson, *Innovation in Wind Turbine*, 1st edn. (John Wiley & Sons, 2011)
8. M.O.L. Hansen, N.N. Sørensen, R.G.J. Flay, Effect of placing a diffuser around a wind turbine. *Wind Energy Int. J. Progress Appl. Wind Power Conver. Technol.* **3**(4), 207–213 (2000)
9. B.L. Gilbert, K.M. Foreman, Experiments with a diffuser-augmented model wind turbine. *J. Energy Res. Technol.* **105**, 46–53 (1983)
10. R.E. Wilson, P.B.S. Lissaman, S.N. Walker, Applied aerodynamics of wind power machines (University of Oregon, 1976)
11. J. Tangler, J.D. Kocurek, Wind turbine post-stall airfoil performance characteristics guidelines for blade-element momentum methods. in *43rd AIAA Aerospace Sciences Meeting and Exhibit* (Reno, Nevada, 2005, January), pp 10–13
12. C. Anderson, *Wind turbines: Theory and practice* (Cambridge University Press, 2020)
13. K. Abe, M. Nishida, A. Sakurai, Y. Ohya, H. Kihara, E. Wada et al., Experimental and numerical investigations of flow fields behind a small wind turbine with a flanged diffuser. *J. Wind Eng. Ind. Aerodyn.* **93**(12), 951e70 (2005)
14. Y. Ohya, T. Karasudani, A. Sakurai, K.-I. Abe, M. Inoue Development of a shrouded wind turbine with a flanged diffuser. *J. Wind Eng. Ind. Aerodyn.* **96**(5), 524e39 (2008)
15. Y. Ohya, T. Karasudani A shrouded wind turbine generating high output power with wind-lens technology. *Energies* **131** (2010)
16. S. Rajakumar, D. Ravaindran, Computational fluid dynamics of wind turbine blade at various angles of attack and low Reynolds number. *Int. J. Eng. Sci. Technol.* **2**(11), 6474–6484 (2010)
17. K. Abe, H. Kihara, A. Sakurai, M. Nishida, Y. Ohya, E. Wada, K. Sato, An experimental study of tip-vortex structures behind a small wind turbine with a flanged diffuser. *Wind Struct.* **413–417** (2006)
18. W.X. Wang, T. Matsubara, J.F. Hu, S. Odahara, T. Nagai, T. Karasutani, Y. Ohya, Experimental investigation into the influence of the flanged diffuser on the dynamic behavior of CFRP blade of a shrouded wind turbine. *Renew. Energy* **78**, 386–397 (2015)
19. Y. Ohya, T. Karasudani, A shrouded wind turbine generating high output power with wind-lens technology. *Energies* **3**, 634–649 (2010)

20. J.-F. Hu, W.-X. Wang, Upgrading a shrouded wind turbine with a self-adaptive flanged diffuser. *Energies* **8**, 5319–5337 (2015). <https://doi.org/10.3390/en8065319>
21. M.M. Hossain, M.H. Ali, Future research directions for the wind turbine generator system. *Renew. Sustain. Energy Rev.* **49**, 481–489 (2015)
22. M.O.L. Hansen, *Aerodynamics of Wind Turbines*, 2nd edn. (Earthscan, London, UK)
23. D. Marten, J. Wendler, G. Pechlivanoglou, C.N. Nayeri, C.O. Paschereit, QBLADE: an open source tool for design and simulation of horizontal and vertical axis wind turbines. *Int. J. Emerg. Technol. Adv. Eng. ICERTSD* **3**(3), 264–269 (2013)
24. N. Sorensen, J. Michelsen, S. Schreck, Navier-stokes predictions of the NREL phase vi rotor in the NASA Ames 80 ft by 120 ft wind tunnel. *Wind Energy* **5**(2–3), 151–169 (2002)
25. A. Elyana, E. Abo-Serie, A. Gaylard, Mesh optimisation for ground vehicle aerodynamics. *CFD Lett.* **2**(1), 54–65 (2010)
26. D. Marten, J. Wendler, G. Pechlivanoglou, C.N. Nayeri, C.O. Paschereit, Qblade: an open source tool for design and simulation of horizontal and vertical axis wind turbines. *Int. J. Emerg. Technol. Adv. Eng. (IJETA)* **3**, 264–269 (2013)

Open Access This chapter is licensed under the terms of the Creative Commons Attribution 4.0 International License (<http://creativecommons.org/licenses/by/4.0/>), which permits use, sharing, adaptation, distribution and reproduction in any medium or format, as long as you give appropriate credit to the original author(s) and the source, provide a link to the Creative Commons license and indicate if changes were made.

The images or other third party material in this chapter are included in the chapter's Creative Commons license, unless indicated otherwise in a credit line to the material. If material is not included in the chapter's Creative Commons license and your intended use is not permitted by statutory regulation or exceeds the permitted use, you will need to obtain permission directly from the copyright holder.

